Hindawi
Advances in Civil Engineering
Volume 2024, Article ID 2156337, 13 pages
https://doi.org/10.1155/2024/2156337

Research Article

Numerical and Preliminary In Situ Investigation on Roadway Excavation Using Static Expansion Mechanical Fracturing

Yin Chen,[1,2] Zijun Li,[1] Jian Zhao,[3] and Dan Huang[3]

[1]*School of Resources and Safety Engineering, Central South University, No. 932 Lushan South Road, Changsha, Hunan 410033, China*
[2]*Xinjiang Kalatongke Mining Co., Ltd., No. 1 Jianshe Road Kalatongke Town, Fuyun County, Xinjiang 836107, China*
[3]*Institute of Mining Engineering, BGRIMM Technology Group, No. 22 Beixing Road East, Daxing District, Beijing 102628, China*

Correspondence should be addressed to Dan Huang; bgrimmhd@126.com

Received 25 January 2024; Revised 10 April 2024; Accepted 27 April 2024; Published 8 May 2024

Academic Editor: Piergiorgio Tataranni

This paper introduced a new nonexplosive roadway excavation method, combining the reserved free space technology and the static expansion mechanical fracturing technology, where the former is implemented by the gasbag, while the piston splitter is for the latter. The numerical model of roadway excavation was set up via PFC3D to investigate the mechanical fracturing performance, including the single-hole fracturing and the hole network fracturing. The results show that the reasonable hole margin is about 1.0–1.5 m, and the optimal column spacing of the hole network pattern is 1.0 m, after comprehensively analyzing the fracturing performance and the splitting force evolution. Moreover, the mechanical fracturing excavation method was applied to construct a parking chamber in the Kalatongke Mine, to preliminarily verify the feasibility of the static expansion mechanical fracturing technology. The in situ investigation results indicate that the excavation footage is about 0.8 m with the piston splitter when adopting a hole margin of 1.0–1.5 m. To sum up, the preliminary field application and the numerical simulation result both support the feasibility of mechanical fracturing, and the reasonable fracturing hole margin is about 1.0 m.

1. Introduction

At present, the drilling–blasting method is still the most common roadway excavation method in underground metal mines all over the world, as a relatively mature technology [1–3]. However, the drilling–blasting construction is a labor- and time-consuming operation [4], and it will produce a great many fractures in the surrounding rock of roadway and stope [5–7]. As the rock blasting within the excavation, it is bad for roadway supporting [8, 9]. In addition, the rock blasting is often accompanied by flyrock, rock vibrations, air overpressure, overbreak, gas emissions, and high-concentration dust [10–12]. These phenomena have a significant influence on mining safety, working environment, and the stability of adjacent backfill and stope [7]. What is more, since the safety risk management and environmental protection policies are getting stricter in China [13, 14], the application of the drilling–blasting method will be gradually restricted, especially for roadway excavation in the ecologically fragile area of China, for example, in Xinjiang and Tibet. The rock breaking and roadway excavation method has been proven in recent years, such as using air–water coupling blasting [15], water jet-assisted rock breaking [16], hydraulic fracturing [17], and so on, but these technologies have a huge of water consumption, which is not in line with the principle of environmental friendly operating standards.

To overcome the drawbacks of existing conventional roadway excavation methods and improve the efficiency of rock breaking, several modern nonexplosive rock breaking approaches have been developed, such as hydraulically driven mechanical splitting (or mechanical fracturing) methods and expansive chemical agents [18], while the former method has a wider application because of its reusability, higher economy, and faster generation of expansive pressure. In terms of the development of mechanical fracturing equipment, it generally includes two main stages: radial splitter stage [19, 20] and piston splitter stage [18]. These two types of equipment are both mainly made of three parts: a hydraulic pump station, oil pipelines, and splitting bars. Whereas the splitting bar of the

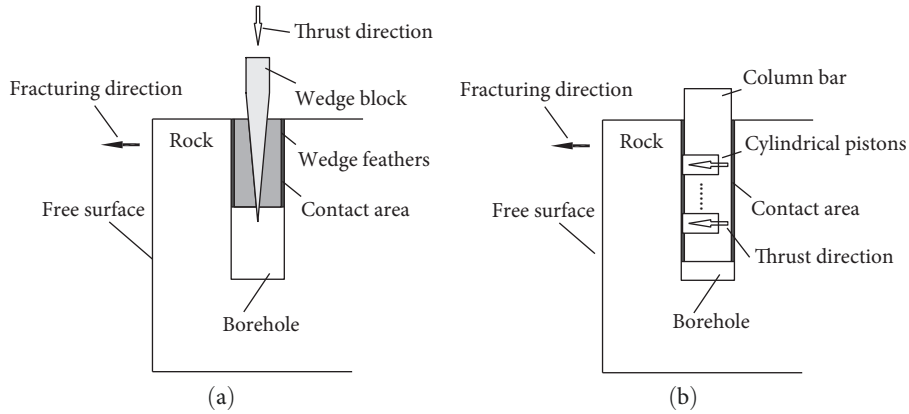

Figure 1: Two types of hydraulically driven mechanical splitting bars: (a) radial splitter and (b) piston splitter.

radial splitter consists of wedge block and two wedge feathers, the splitting bar of the piston splitter is mainly composed of column bar and multiple cylindrical pistons, as shown in Figure 1. The work process of mechanical fracturing using a radial splitter starts a hole drilling, then the pump station provides high-pressure oil to the splitting bar through hydraulic oil pipelines to push the wedge block to move downward, and then the wedge block drives the wedge feathers to expand. In this process, the axial thrust is converted into the radial splitting force for the borehole wall [21]. When the splitting force is large enough, the rock will be fractured toward the side of the free surface. As for the work process of the piston splitter, most of the steps are similar to that of the radial splitter, but the high-pressure oil is directly pumped into the column bar to jut out multiple cylindrical pistons toward the free surface. Then the cylindrical pistons apply a horizontal thrust on the borehole wall to break the rock.

Due to the significant advantages of mechanical fracturing, many scholars have considered it the primary roadway excavation method and carried out lots of basic research [18]. Li et al. [21] studied the effect of auxiliary holes by comparing the rock breaking performance using a hydraulic splitter under the situation with and without auxiliary holes, based on the numerical simulation results of finite element method (FEM) and experimental results. When the auxiliary holes are located at the prefabricated angles $\alpha = 40°$ and 45°, the crack propagation can be well induced, and the cracks pass through the auxiliary holes. Liu et al. [22] studied the rock breaking performance of rock specimens using a radial splitter and revealed the crack propagation during the rock breaking by numerical simulation approaches via AUTODYN code; besides, they concluded that the borehole margin, confining pressure, borehole depth, and borehole diameter are the main factors influencing on rock breaking. Zhou et al. [23] experimentally investigated the fracture performance with a single borehole by using a hydraulic splitter, and they also studied the effect of the rock compressive strength, confining pressure, and borehole margin, and then they summarized the peak fracture pressure with the free surface is lower than that without the free surface. What is more, de Graaf and Spiteri [24] introduced a successful application case of the hydraulic splitting cylinder (that is, radial splitter) for breaking rock at the Goldfields KDC West Gold Mine in South Africa, and they proposed that the splitter becomes more effective once the second free face is presented; therefore, they thought that future work should concentrate on developing more effective techniques for creating an initial cut.

The above existing researches mainly focus on the utilization of radial splitter. However, with the development of new mechanical rock breaking equipment, the piston splitter has more outstanding rock breaking ability and higher rock breaking efficiency. The rock breaking depth of the radial splitter is generally hundreds of millimeters, while it is more than 1 m for the piston splitter. Furthermore, the most current investigations on rock breaking performance adopt laboratory experiments and numerical simulations with small-scale rock specimens, which is difficult to directly guide the fieldwork. In addition, the numerical simulation based on FEM cannot answer the accurate range of rock fractures and fragments.

To realize the transformation of roadway excavation from the explosive method to the nonexplosive method in underground metal mines, this paper presents a new excavation method based on the static expansion mechanical fracturing and the gasbag reserved free space technologies. In this work, the engineering background and the operation of the new mechanical fracturing excavation method are introduced, and then the fracturing properties of a single hole and hole networks are investigated using the distinct element method (DEM) via PFC3D code. Finally, the field application of mechanical fracturing with the piston splitter in the Kalatongke Copper–Nickel Mine is carried out.

2. Engineering Background

2.1. Geology Information. The Kalatongke Mine is located about 500 km north of Urumqi, Xinjiang. The copper–nickel lode consists of three ore deposits, as shown in Figure 2, and their maximum depth is about 600 m, where the elevation level of the ground surface is about 1,000 m. The mining method in the 1# and 2# deposits are mainly the downward cut-and-fill method and the sublevel open stoping with subsequent backfilling method for the 3# deposit. The uniaxial

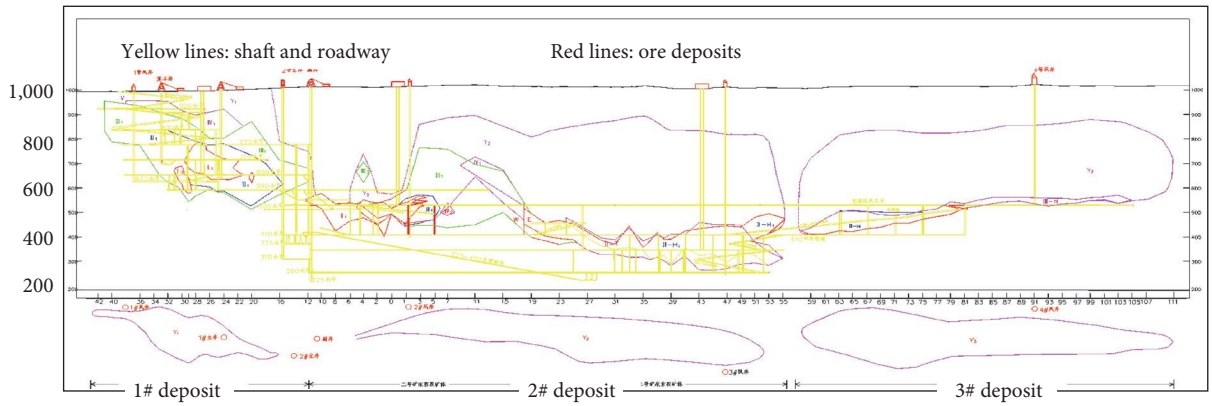

Figure 2: Development system of the Kalatongke Mine.

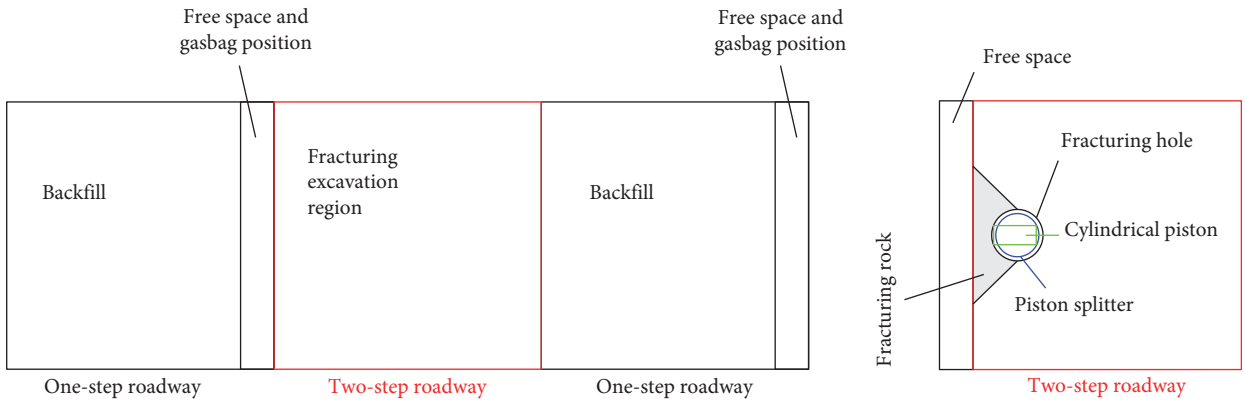

Figure 3: A new roadway excavation method: (a) gasbag reserved free space in the two-step roadway and (b) static expansion mechanical fracturing technology.

compression strength of the ore body is about 140 MPa, while 110–140 MPa is for the surrounding rock.

2.2. New Roadway Excavation Method

2.2.1. Gasbag Reserved Free Space Technology. For the drilling–blasting method, the sufficient free surface is an important factor for successful blasting excavation, which is generally realized through constructing the cut and auxiliary holes on one side of the roadway [25]. In this process, however, a great deal of time is spent on the construction of the blasting cut, resulting in a lower excavation efficiency. Therefore, we proposed a new method to form a free surface by setting gasbags in the backfill of the one-step mining area. It cannot only be used for the drilling–blasting method but also the mechanical fracturing excavation method.

In detail, after the one-step mining in the ore body, the gasbags are placed on the roadway side along the roadway axis and then backfilling the one-step roadway and stope. When excavating the two-step roadway, the gasbag is deflated and recycled, thereby forming a reserved free space in the gasbag region, as shown in Figure 3(a). It makes sure that the rock mass inside the two-step roadway is under uniaxial compression, which is helpful for the two-step roadway excavation. Meanwhile, the gasbag reserved free space technology also saves the construction cost of the free surface, with cost savings of about 50%.

2.2.2. Static Expansion Mechanical Fracturing Technology. Due to the high rock hardness, the feasibility of a cantilever roadheader applied in the Kalatongke Mine is low. Thus, after creating an initial cut with gasbag reserved free space technology, the roadway excavation could be accomplished through the static expansion mechanical fracturing technology (see Figure 3(b)), using the piston splitters mentioned in Figure 1(b).

In detail, the fracturing holes are first set up inside the roadway excavation region near the initial cut, the depth of which is about 1.0 m, about 100–200 mm for the diameter. The specific borehole diameter is determined by the overall dimension of the selected piston splitter, and it is slightly larger than that of splitter in general. Then the piston splitter is inserted into the boreholes, and multiple cylindrical pistons are jut out from the piston splitter subsequently. As the travel of pistons increases, the splitting force acting on the surrounding rock of the fracturing hole improves continuously, as well as more and more microcracks in rock mass. When the splitting force reaches a certain critical value, the roadway rock mass near the initial cut is fractured, and then a new free surface appears, which is used for the next

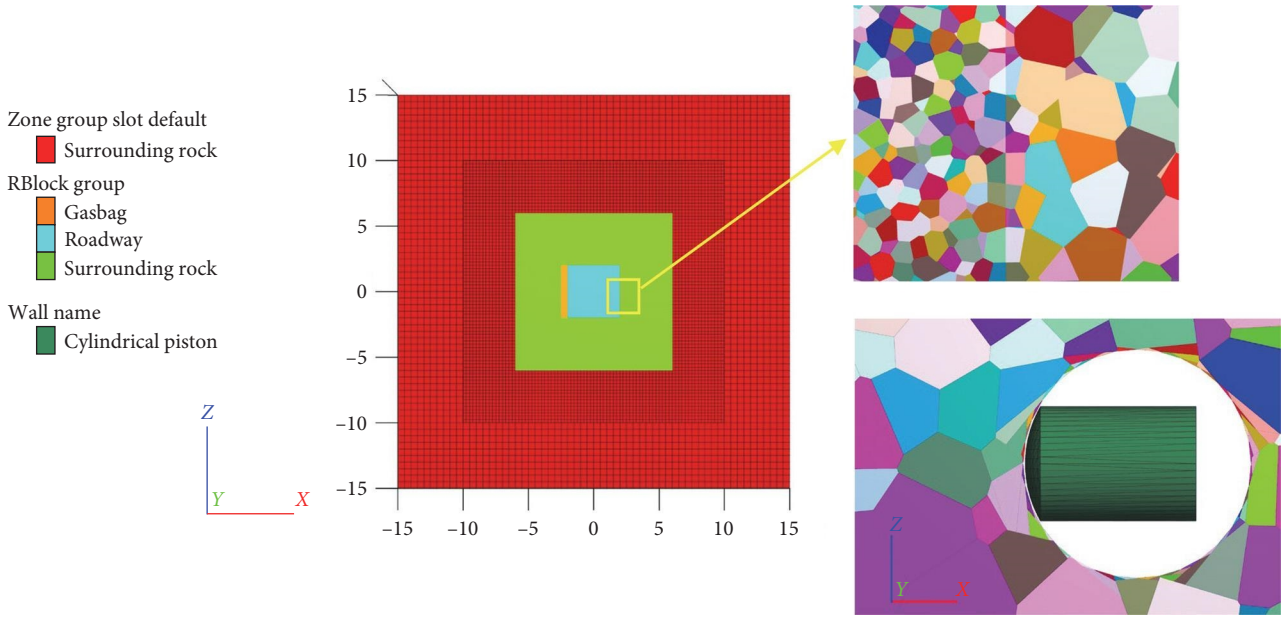

Figure 4: Roadway excavation numerical model with gasbag reserved free space.

fracturing excavation cycle. The maximum splitting force of the adopted piston splitter is about 25 MN and with a maximum piston travel of 30 mm.

3. Numerical Analysis on Mechanical Fracturing

3.1. Model Setup. To make sure the successful application of the static expansion mechanical fracturing excavation in the Kalatongke Mine, it is necessary to design reasonable spacing pattern parameters of the hole network. In this section, hence, a roadway excavation numerical model is set up using PFC3D to investigate the rock breaking performance, including the range of rock fragments, rock fractures, and the splitting force. The numerical model includes two parts, continuum-based zone element and discontinuum-based rigid block element, as shown in Figure 4. The blocks and zones are connected through wall elements, and the zone elements are regarded as the surrounding rock of block elements, while the block elements are divided into three regions: surrounding rock, gasbag space, and roadway excavation region.

To speed up the numerical calculation, the excavation process is simplified into a plane strain model. And the spacing of cylindrical pistons along the piston splitter is 0.3 m, so the numerical model is set to 0.3 m thick in consideration of the symmetry effect between cylindrical pistons. The geometry size of the numerical model is 30.0 m × 0.3 m × 30.0 m ($X \times Y \times Z$). Where, the roadway is 4.0 m × 4.0 m ($X \times Z$), and the size of the reserved space formed by the gasbag on the left side of the roadway is 0.5 m × 4.0 m ($X \times Z$). The numerical model has a total of approximately 30,000 block elements and about 30,000 zone elements, and their minimum size is about 25 mm. In general, the smaller the block element size, the more accurate the simulated fragment range. But it also means more block elements and lower calculation efficiency, if adopting a smaller block element size. While if adopting a larger element size, the simulated broken rock blocks will not conform to the actual engineering situation. The constitutive model of the zone element-based surrounding rock is an ideal elastic model, and the contact material model of the block is soft bond. The contact model between cylindrical piston and rock mass is linear model. Table 1 shows the mechanical parameters of the numerical model.

According to the geological information of the Kalatongke Mine, the depth of roadway is about 400 m, and the lateral stress coefficient of rock mass around the roadway is assumed as 0.5. The bottom boundary of the numerical model is fixed, and the vertical and horizontal stresses based on the self-weight of overburden and lateral stress coefficient are applied on the top surface and four sidewall surfaces as supplementary stress. After reaching the first initial stress equilibrium of the numerical model, the blocks inside the gasbag space and boreholes are deleted, where the borehole diameter is 220 mm, and then the numerical model with free space is calculated to reach a new initial stress equilibrium, which is considered as the initial state before mechanical fracturing. Finally, to carry out the mechanical fracturing, a cylindrical piston is generated inside each borehole by the wall element (see Figure 4), the diameter of which is 110 mm. After comprehensive considering the quasi-static equilibrium state of rock mass and reasonable numerical calculation time, the cylindrical piston is applied a constant horizontal velocity of 10 m/s to move toward the free space, and the travel distance is about 30 mm. To sum up, the flow diagram of mechanical fracturing numerical simulation is shown in Figure 5.

3.2. Single-Hole Mechanical Fracturing

3.2.1. Single-Hole Layout Scenario. It is helpful to design the spacing pattern parameters of the hole network after figuring

Table 1: Mechanical properties of numerical model.

Parameter	Zone	Block	Bond contact
Elastic modulus	65 GPa	—	65 GPa
Poisson	0.26	—	—
Density	2,990 kg $(m)^3$	2,990 kg $(m)^3$	—
Friction coefficient	—	—	0.5
Normal-to-shear stiffness ratio	—	—	2.0
Friction angle	—	—	47°
Cohesion	—	—	20 MPa
Tensile strength	—	—	5 MPa

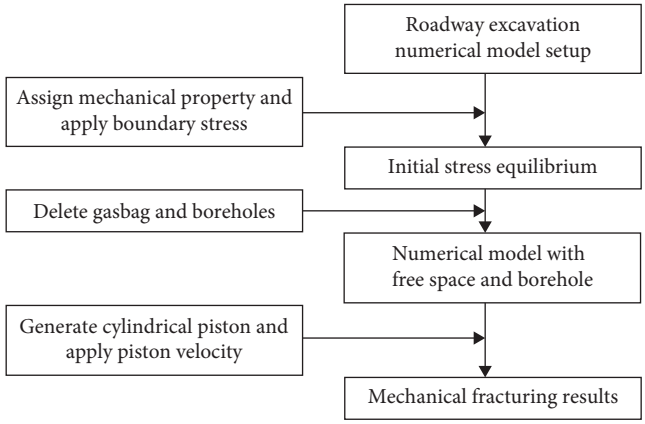

Figure 5: Flow chart of mechanical fracturing numerical model.

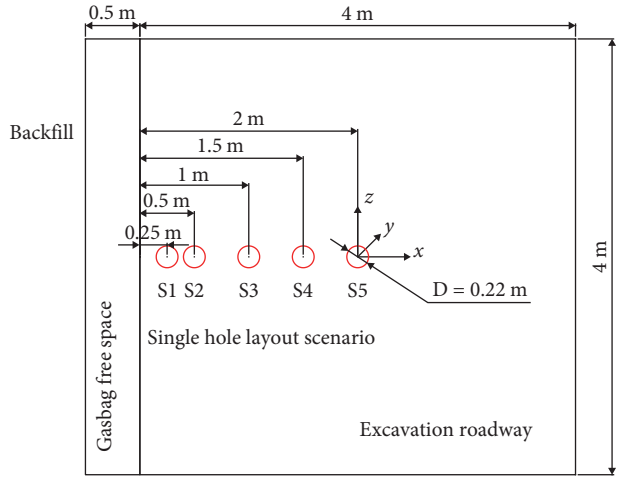

Figure 6: Layout scenario of single-hole mechanical fracturing.

out the rock breaking performance of mechanical fracturing with a single hole, so the mechanical fracturing performance of a single hole is firstly investigated. The borehole layout includes five scenarios, S1–S5. Their vertical positions are the same, all located on the horizontal center line. But the horizontal positions are different; the margin to the free surface varies from 0.25 to 2.0 m, as shown in Figure 6.

As the hole margin increases, to successfully break the rock mass, it needs to produce a longer fracture between the fracturing hole and the free surface, as well as a higher splitting force on the borehole wall. For an extremely large margin, the fracture induced by the mechanical fracturing may not propagate to the free surface, causing the failure of mechanical fracturing. Apart from the range of rock fracture and fragment, the splitting force between the cylindrical piston and the borehole wall is also an important factor. If the simulated maximum splitting force is beyond the rated splitting force of the piston splitter, even though the fracture can propagate to the free surface, the corresponding margin is still not suitable. Therefore, to decide the reasonable margin, it mainly compares the rock breaking effect and splitting force under different margin scenarios by the numerical simulation of single-hole mechanical fracturing.

3.2.2. Single-Hole Fracturing Results. According to the numerical simulation results of the single hole, the mechanical fracturing performance in different scenarios is summarized in Table 2. And Figure 7 shows the evolution of the rock fragment area and the maximum splitting force of the piston splitter.

It can be seen from Table 2 and Figure 7 that the fracture area continuously improves as the hole margin increases, and the fracture shape gradually changes from a triangle to a rectangle. But when the margin is too large, as in scenario 5 ($X = 2.0$), the fractures are unable to penetrate the rock mass from the fracturing hole to the free surface, so the corresponding margin pattern is not feasible. Moreover, the maximum splitting force also gradually rises as the hole margin in general. Among them, the maximum splitting forces in S1, S2, S3, and S4 are all below the rated force, where the FR-200 piston splitter used at the Kalatongke Mine has a rated splitting force of about 2,500 tons, that is, 25 MN, while the maximum splitting force in S5 is much larger than the rating value.

The rock fragment and fracture induced by mechanical fracturing in different single-hole scenarios are shown in Figures 8 and 9. The former indicates the rock macrofragment range while the rock microfracture inside the rock fragment range for the latter. In Figure 8, the fragment range is determined by the contact state of the rock block element. When bonded contacts between block elements failure, it forms rock macrofragments, while the color represents the fragment ID. Figures 8 and 9 reveal that the overall rock breaking effect by single-hole mechanical fracturing first increases and then decreases as the hole margin increases based on the numerical simulation results. When the hole

Table 2: Fracturing performance of single hole.

Scenario	Fracture penetrability	Fracture shape	Fragment area (m^2)	Max. splitting force (MN)
S1 ($X = 0.25$ m)	Yes	Triangle	0.125	3.4
S2 ($X = 0.5$ m)	Yes	Triangle	0.5	8.2
S3 ($X = 1.0$ m)	Yes	Trapezoid	1.875	22
S4 ($X = 1.5$ m)	Yes	Square	2.25	18
S5 ($X = 2.0$ m)	No	Rectangle	2.47	32

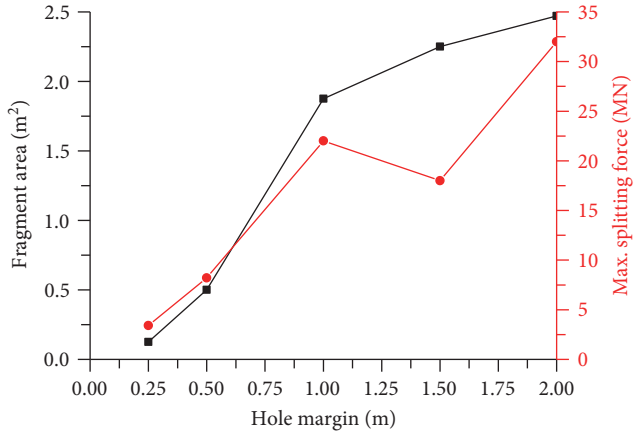

Figure 7: Fracturing performance evolution of single hole as hole margin.

margin between the crack hole and the free surface is within a reasonable range, the rock fractures during the single-hole mechanical fracturing can penetrate to the free surface. And with the increase of the hole margin, the ranges of rock fragment and fracture continue to expand. However, when the hole margin exceeds the critical margin, the rock fragment and fracture cannot extend to the free surface, causing the failure of the mechanical fracturing. In addition, Figure 9 also illustrates that the rock failure is mainly tensile failure in the process of splitting rock mass. The green fractures in Figure 9 represent the tensile failure state of the contact elements between fragment block elements, and the tensile or shear fractures are determined by the contact state between block elements. The microfractures appear between macrofragment blocks, when the contact elements between them happen tensile or shear failures.

Figure 10 presents the relationship between the splitting force of the cylindrical piston acting on the hole wall and the piston travel. It demonstrates that, in general, the splitting force gradually increases, and then decreases after reaching the peak value, with the increase in the travel of the cylindrical piston inside the column bar. Generally speaking, the travel corresponding to the peak splitting force increases in the hole margin, but in special circumstances, the maximum splitting force in scenario 4 ($X = 1.5$ m) is slightly less than that in scenario 3 ($X = 1.0$ m), also presented in Figure 7; the reason is that the splitting force in the hole margin of 1.5 m does not reach the peak value within 30 mm of the cylindrical piston travel. That is, when the hole margin $X \leq 1.0$ m, the splitting force can reach the peak value within 30 mm travel while not for the hole margin $X \geq 1.5$ m.

Then to determine the reasonable margin by the single-hole fracturing results, it should comprehensively analyze the rock breaking effect and the maximum splitting force required. On the one hand, if the single-hole margin is small, the maximum splitting force required and the corresponding piston travel are also smaller, which is conducive to lowering the performance requirement for the piston splitter and then further facilitating the popularization and application of the hydraulic driven mechanical fracturing technology. But if using a small spacing pattern for the hole network, there is a disadvantage of more borehole drilling construction, which increases the drilling cost and the utilization number of piston splitters. What is more, for the small spacing pattern, the peaking force appears within a small travel, like the single-hole margin of 0.25 and 0.5 m mentioned in Figure 10, and the splitting capacity of the piston splitter is wasted.

On the other hand, however, if the single-hole margin is big, the fractures produced by the mechanical fracturing cannot expand to the initial free surface of the gasbag reserved free space effectively, so there is a risk of fracturing failure. Furthermore, even if the range of the rock fracture can propagate to the free surface while the required maximum splitting force is over the rated splitting capacity of the equipment, it also cannot effectively break the rock to achieve the roadway excavation by the static expansion mechanical fracturing technology.

According to the numerical simulation results, and combined with the above analysis, the critical hole margin is 1.5 m, and the reasonable hole spacing should be 1.0–1.5 m. In this range, it can make full use of the rated splitting force of the piston splitter used in the Kalatongke Mine, and the hole number construction is suitable. It should be noted that if the initial crack of the rock mass is rich, and the stress of the surrounding rock mass is small, it can select 1.5 m as the reasonable hole space parameter of the hole network in the process of in situ mechanical fracturing. If the rock mass has a poor initial crack, a high strength, and high stress, then a space parameter of 1.0 m is a better choice.

3.3. Hole Network Mechanical Fracturing

3.3.1. Hole Network Layout Pattern. In this section, two kinds of layout patterns of the mechanical fracturing hole networks are designed, because of the reasonable single-hole margin of 1.0–1.5 m, as presented in Figure 11. These two patterns are both arranged in a straight line and column, and this study only investigates the fracturing effect of the split holes while ignoring the guiding function of the auxiliary holes around the roadway profile contour and between the split holes.

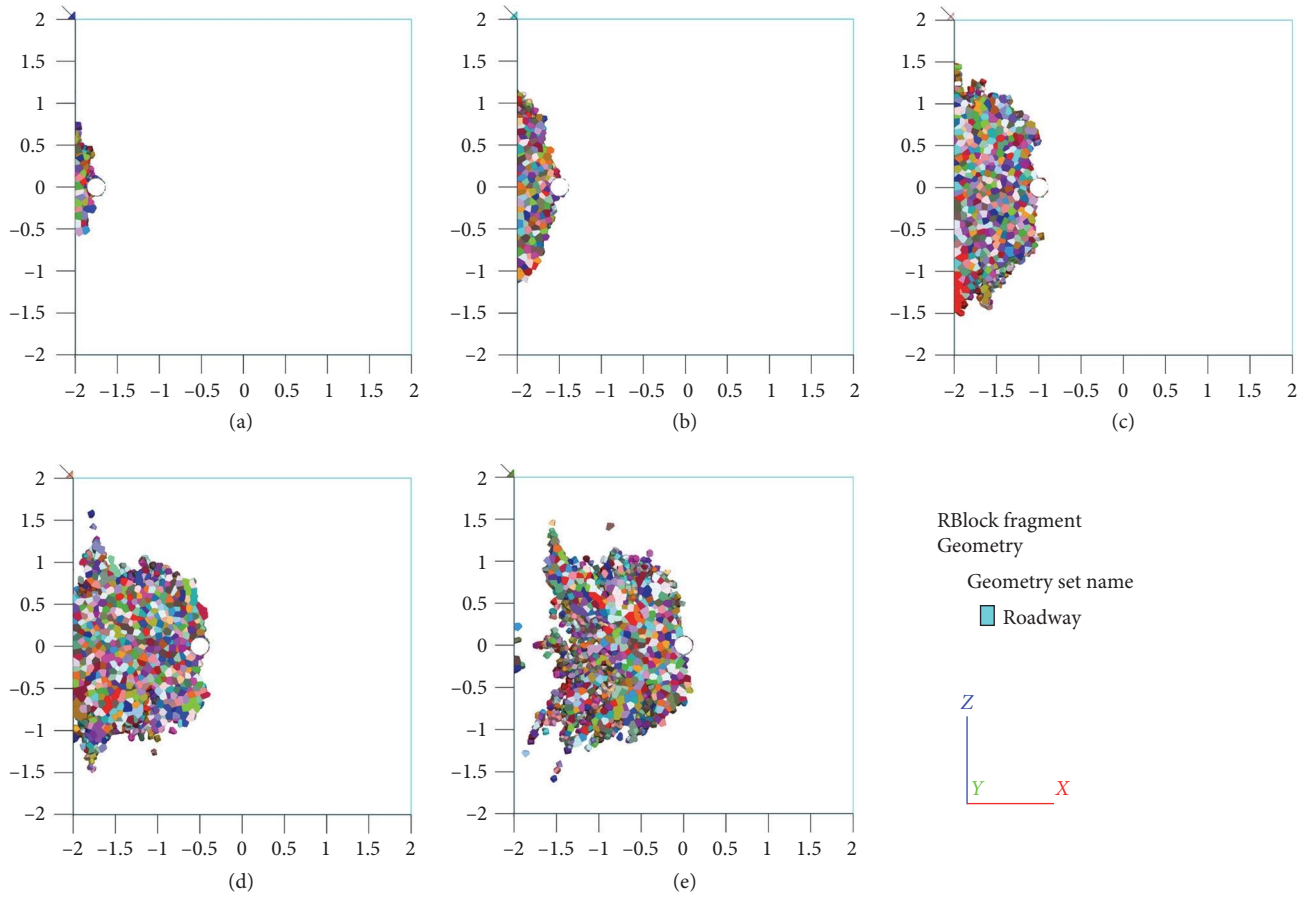

Figure 8: Rock macrofragment range inside the roadway excavation area induced by single-hole mechanical fracturing: (a–e) stands for scenario of S1–S5.

Pattern 1 is a total of 12 split holes in four columns, with a column spacing of 1.0 m and a column spacing of 1.25 m. There are three split holes in each column, top, center, and bottom hole; they are carrying out mechanical fracturing at the same time. While there are a total of nine split holes in three columns for pattern 2, the column and row spacing are 1.0 and 12.5 m.

The quantity difference in split holes for the two patterns is negligible in each excavation cycle, so their borehole drilling construction cost and roadway excavation efficiency are similar and are both better than the drilling–blasting method. Compared with pattern 1, as the column spacing of the hole network keeps increasing, the required splitting force of pattern 2 accordingly improves, also for the piston travel corresponding to the peak splitting force. And the failure risk of mechanical fracturing using pattern 2 is higher than pattern 1 because the column spacing of 1.5 m is the critical hole margin of the single hole. On the other hand, however, regardless of pattern 1 or pattern 2, the splitting capacity of the piston splitter is fully utilized. Therefore, the comparison of their pros and cons mainly concentrates on the roadway section forming result, the overbreak and underbreak situation, and the maximum splitting force.

3.3.2. Hole Network Fracturing Results. Table 3 presents the comparison results of the different hole network patterns, based on the mechanical fracturing numerical simulation results. The value of overbreak or underbreak is determined via measuring the distance of rock breaking range beyond or short of the roadway design profile. Table 3 makes it clear that both hole network patterns can fracture the rock to form a square roadway with a side length of 4.0 m, and the required maximum splitting force in each fracturing hole is generally within the rated splitting force of the piston splitter. But for pattern 2, the maximum splitting force is slightly greater than the rated splitting force, which may cause the failure of the mechanical fracturing. In addition, there is a certain overbreak and underbreak for the excavation roadway by both patterns (Figure 12). Whereas the overbreak mainly appears in the roof and floor region, the underbreak is in the right side of the last column of the fracturing hole. The maximum size of the roadway overbreak and underbreak is about 0.3 m. Therefore, to make sure the success of the mechanical fracturing and reduce the roadway overbreak, it is necessary to set some auxiliary guiding holes and additional fracturing holes, according to the in situ construction situations and the actual mechanical fracturing results.

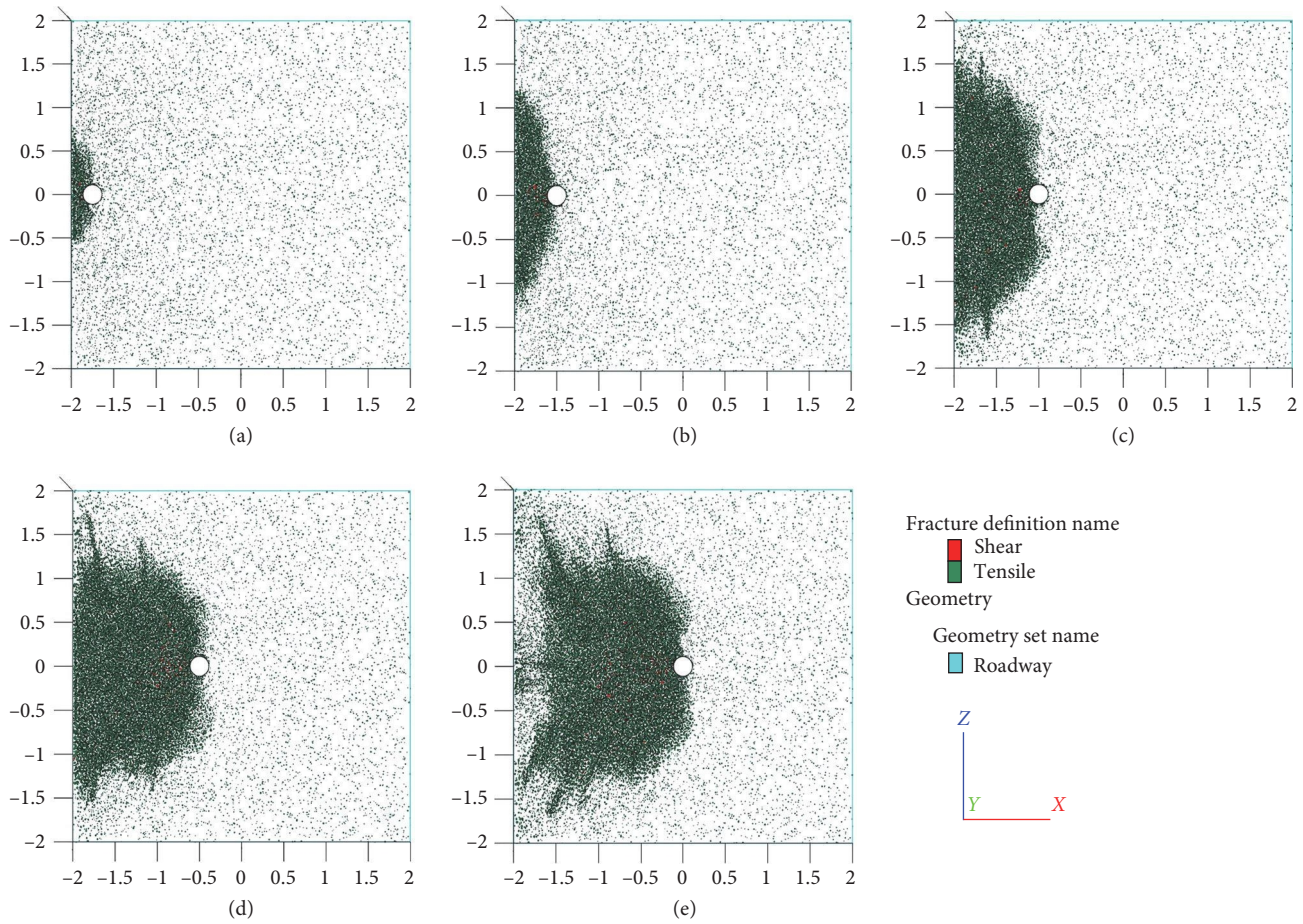

Figure 9: Rock microfracture range inside the roadway excavation area induced by single-hole mechanical fracturing: (a–e) stands for scenario of S1–S5.

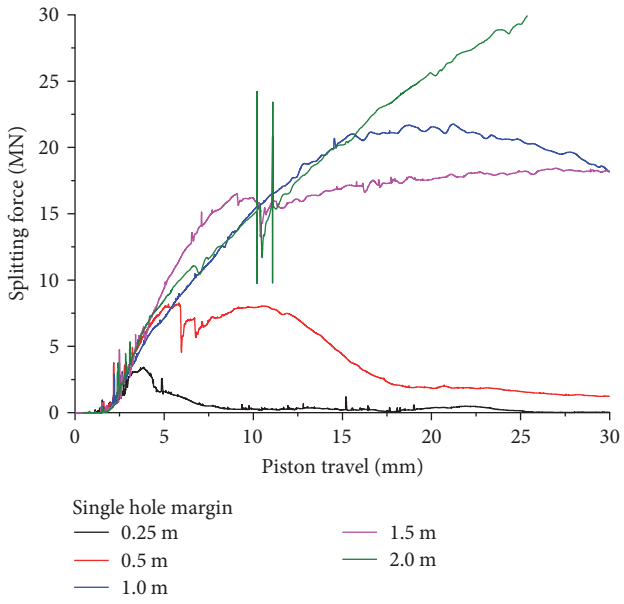

Figure 10: Splitting force by single-hole mechanical fracturing.

Figure 12 exhibits roadway section forming results by the two patterns of the hole network mechanical fracturing, where the square with a side length of 4 m is the roadway design profile. The rock fragment induced by mechanical fracturing can cover the entire roadway section range, which proves the feasibility of the new excavation method based on the gasbag reserved free space and the static expansion mechanical fracturing technologies. In the aspect of the roadway overbreak, the overbreak in the floor is bigger than that in the roof, and the overbreak by pattern 1 of 1.0 m column spacing is slightly bigger than pattern 2 of 1.5 m column spacing. And the overbreak is mainly distributed in the region between the first column and the second to the last column of the fracturing hole, which is mainly produced in the last few columns. Hence, it is necessary to clean the fractured rock mass in time, after the mechanical fracturing in the first few columns, to avoid the uncleaned broken rock mass affecting the range of free surface. In addition, the roadway underbreak happens by both patterns, and it only exists on the right side of the roadway after the last column of mechanical fracturing, the range of which is about 100 mm

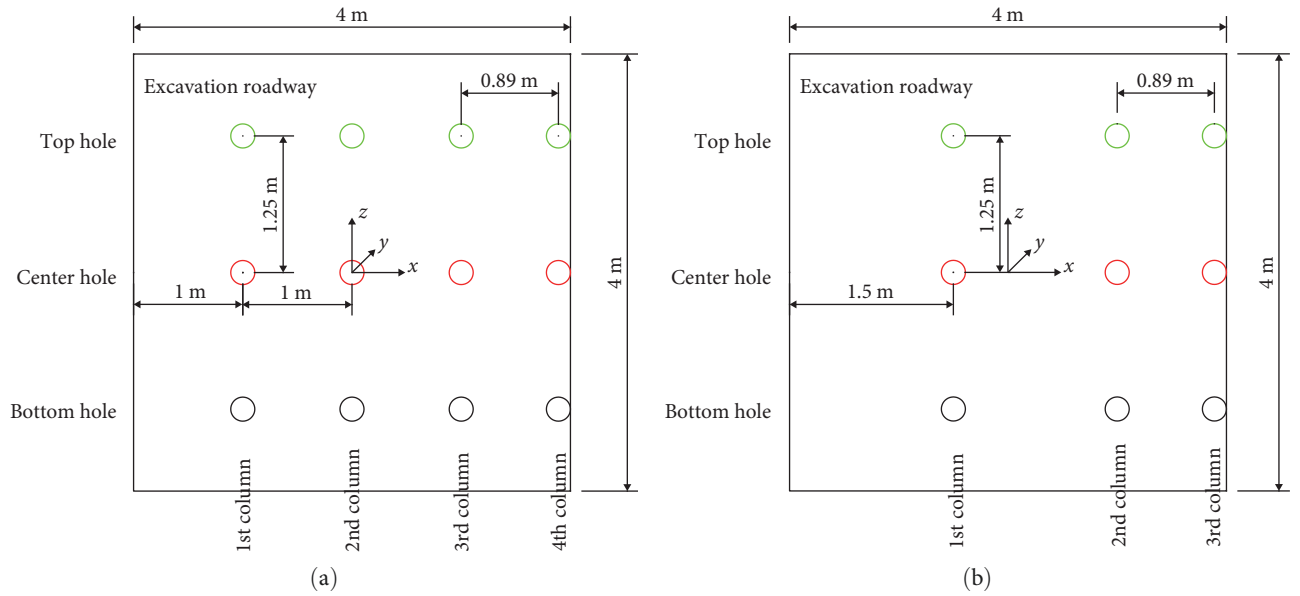

Figure 11: Layout pattern of hole network mechanical fracturing: (a) pattern 1 and (b) pattern 2.

Table 3: Fracturing performance of hole network.

Pattern	Roadway section forming	Max. splitting force range (MN)	Overbreak and underbreak
P1 (column spacing = 1.0 m)	Yes	15–25	Overbreak 0.1–0.5 m, underbreak 0.1–0.3 m
P2 (column spacing = 1.5 m)	Yes	15–28	

on the roadway side, which is close to the radius of the fracturing hole, but a much larger underbreak about 300 mm around the shoulder corner of the roof and floor.

Figure 13 gives the splitting force evolution during the mechanical fracturing for the two hole network patterns. The splitting force of the two patterns with different spacing parameters is generally between 15 and 25 MN. While there is a peak splitting force of 28 MN in pattern 2, it is slightly greater than the rated splitting value, which happens in the first column bottom hole near the roadway floor. Moreover, for pattern 1 with the column spacing of 1.0 m as shown in Figure 13(a), the peak splitting forces of different fracturing holes all appear within the effective travel of 30 mm, and then the splitting force gradually decreases or remains unchanged. However, in pattern 2 with a larger column spacing as presented in Figure 13(b), the splitting force of most of the cylindrical piston continues to increase at the maximum piston travel. On the one hand, the rated splitting force could be fully utilized, but on the other hand, the fractures induced by mechanical fracturing can penetrate the rock mass and propagate to the free surface only if the piston travel is large. There is a risk of cracking failure for pattern 2.

In conclusion, the optimal hole network pattern should take full account of the section size of the roadway, the mechanical properties and stress environment of the roadway and surrounding rock mass, the construction quantity of fracturing holes and auxiliary guiding holes, the operation time of mechanical fracturing, and the overbreak and underbreak conditions after mechanical fracturing, as well as the required maximum splitting force. Based on the numerical simulation results of the hole network mechanical fracturing, it recommends pattern 1 with a column spacing of 1.0 m.

4. Preliminary In Situ Investigation on Mechanical Fracturing

4.1. Preliminary Application Test. To verify the feasibility of mechanical fracturing roadway excavation in the Kalatongke Mine, a preliminary application test was carried out first in constructing the parking chamber near the 770-m level roadway, as shown in Figures 14(a) and 14(b). The free surface is constructed by the core drilling rig (Figure 14(c)), and Figure 14(d) gives the piston splitter. The excavation size of the test roadway is about 5 m wide and 3.2 m high. In addition, another roadway excavation test was conducted at the 926 m level, with the roadway shape and size similar to that of the 770 m level parking chamber.

4.2. Field Application Result. It starts with the construction of initial cut holes and fracturing holes in the mechanical excavation at the 770 m level and the 926 m level, as shown in Figures 15(a) and 15(c). The cut holes are drilled along the chamber and roadway boundary, and the fracturing holes are 1.0–1.5 m from the cut holes. There are about 10 fracturing holes in total in each excavation cycle, and all splitting forces are lower than the rated splitting capacity of piston splitter. The mechanical fracturing results presented in Figures 15(b) and 15(d) reveal that the mechanical fracturing excavation is

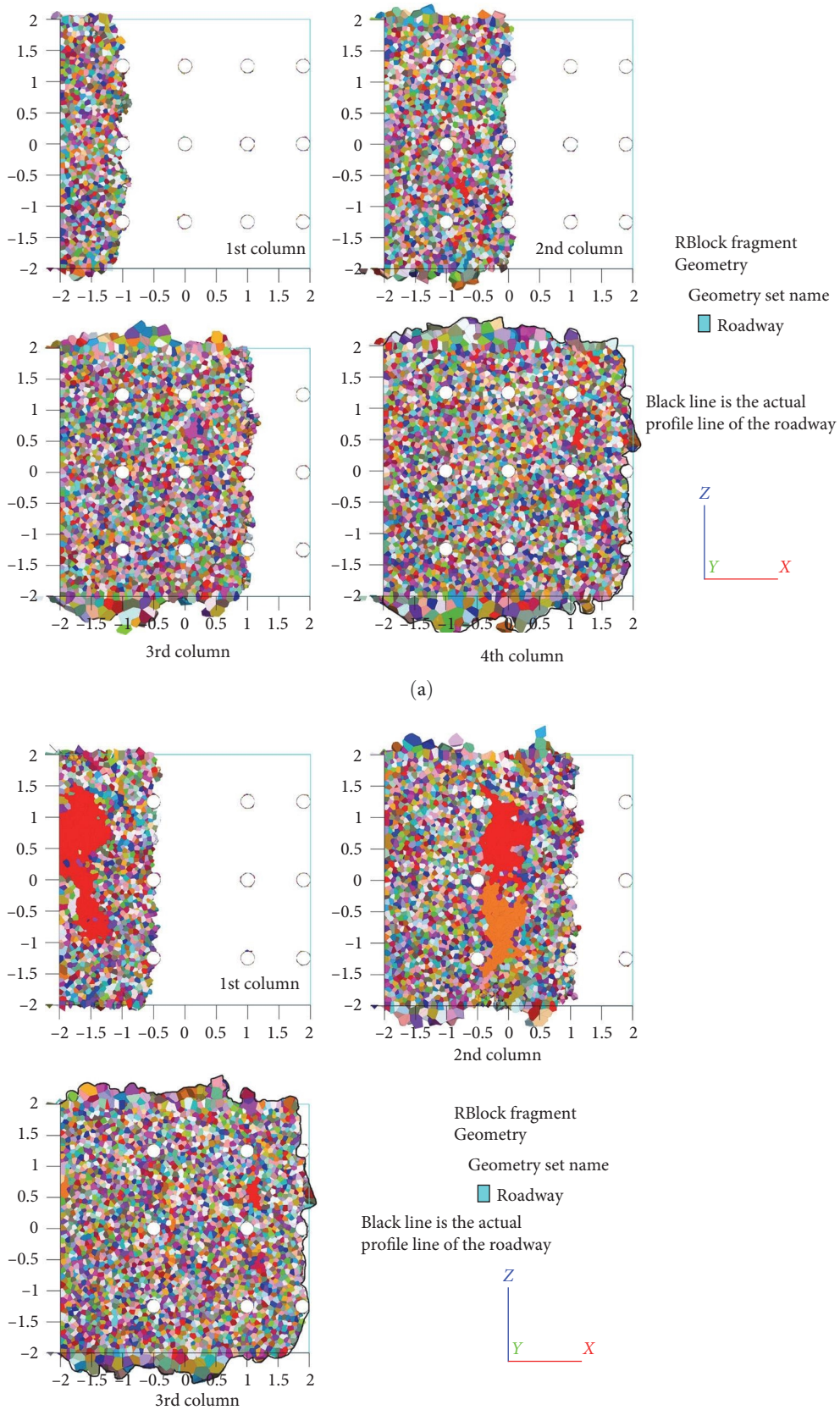

Figure 12: Roadway section formed by hole network mechanical fracturing. (a) and (b) are pattern 1 and pattern 2.

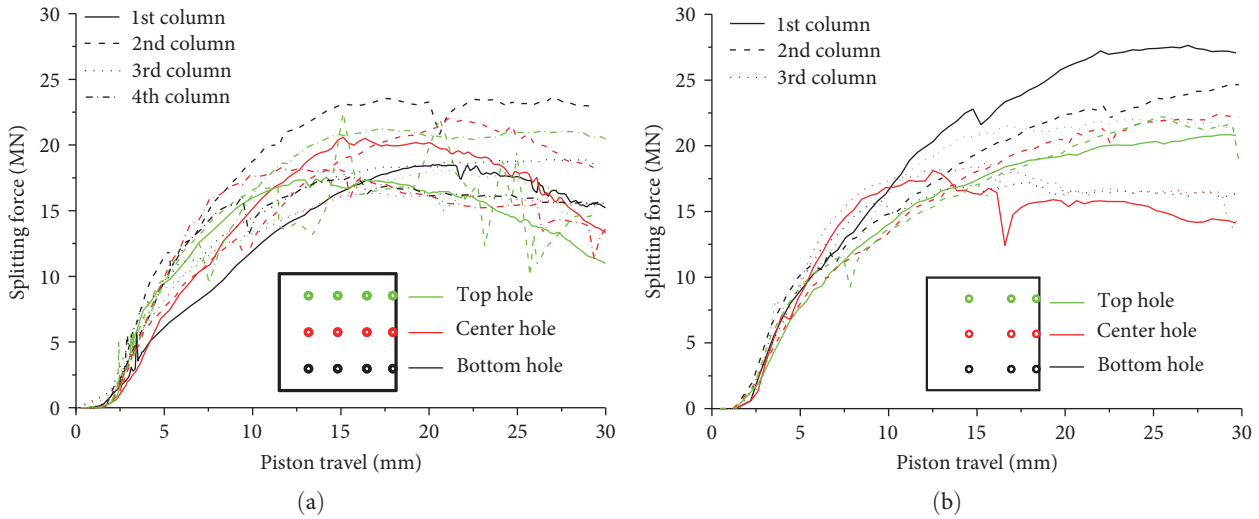

FIGURE 13: Splitting force by hole network mechanical fracturing: (a) pattern 1 and (b) pattern 2.

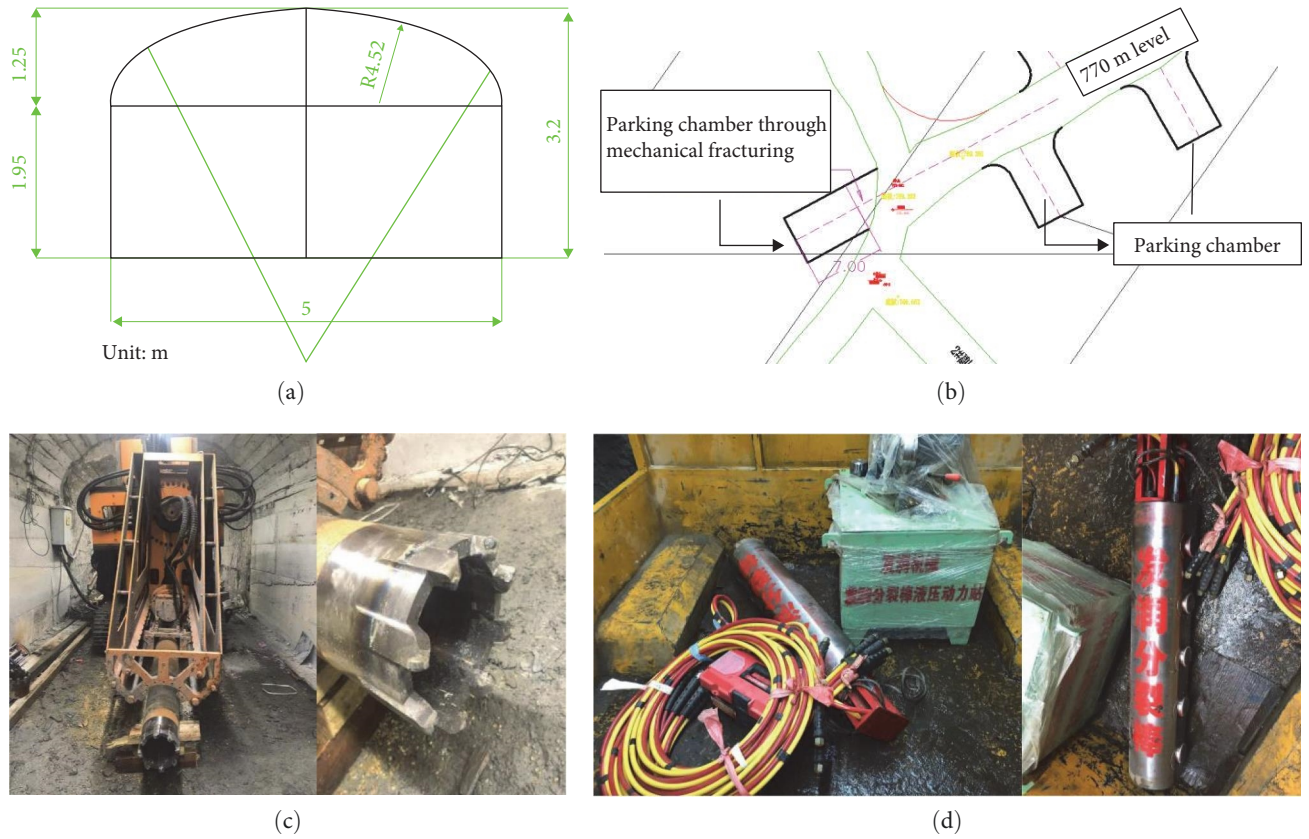

FIGURE 14: Application test of mechanical fracturing roadway excavation: (a) cross-section of parking chamber; (b) parking chamber location; (c) core drilling rig; and (d) piston splitter.

feasible when adopting a hole margin of 1.0–1.5 m, and the effective excavation footage is about 0.8 m in each fracturing cycle. The successful application test in the chamber excavation provides a reliable technical basis for the application of the new roadway excavation method in the Kalatongke Mine.

5. Conclusions

This study introduced a new nonexplosive roadway excavation method based on the gasbag reserved free space and static expansion mechanical fracturing technologies, which overcomes the

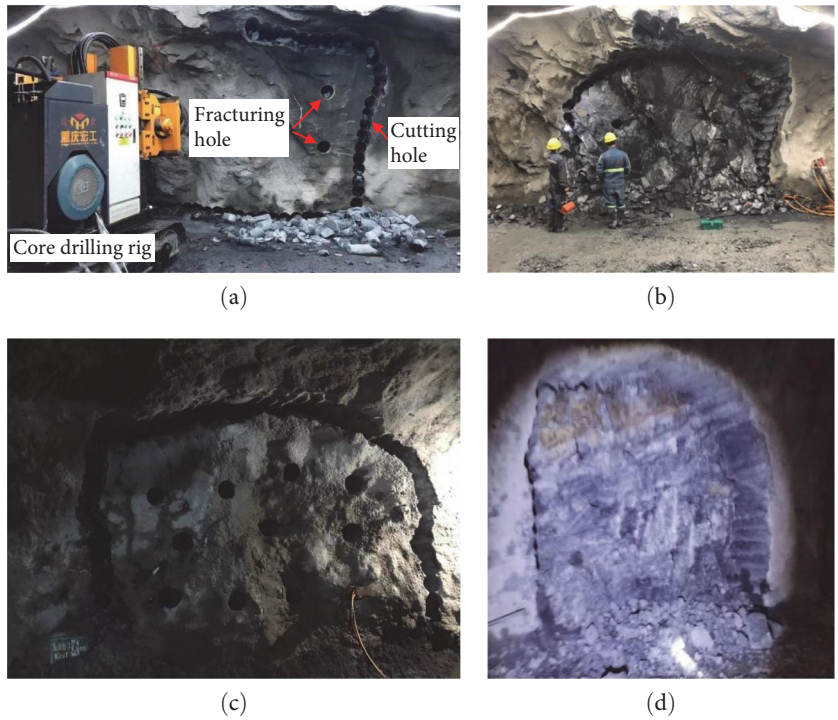

FIGURE 15: Mechanical excavation with piston splitter. (a) and (c) Cut hole and fracturing hole constructions at 770 m level and 926 m level; (b) and (d) static expansion mechanical fracturing results at 770 m level and 926 m level.

disadvantage of the conventional drilling–blasting method. The mechanical fracturing performance was numerically investigated at first, to study the reasonable single-hole margin and the optimal hole network pattern. Then taking the Kalatongke Mine as an example, the application of the new mechanical fracturing method is exhibited to validate the feasibility. The main conclusions are drawn as follows:

(1) The new roadway excavation method includes two implementation phases, setting up free space with reserved gasbag and mechanical fracturing excavation with piston splitter. In the first phase, the gasbag is placed in the one-step roadway near the two-step roadway before backfilling the one-step roadway and stope. In the second phase, the gasbag is deflated and recycled to form an initial cut, and the fracturing hole is constructed at the same time, and then the two-step roadway is excavated through the mechanical fracturing using the piston splitter in the fracturing hole.

(2) The numerical model of roadway excavation was set up via PFC3D to simulate the mechanical fracturing process using the piston splitter. During the mechanical fracturing process, the fractures in rock mass are mainly induced by tensile failure. As the single-hole margin increases, the overall rock fracturing effect first increases and then decreases, and the margins that are too large or too small are not good for efficient mechanical fracturing. There is a reasonable single-hole margin of 1.0–1.5 m, after comprehensively considering the borehole construction quantity, the fracturing area, the required splitting force, and so on.

(3) Two kinds of hole network patterns were designed based on the single-hole results, and then the mechanical fracturing performance was compared. The two patterns with column spacing of 1.0–1.5 m can both form the roadway section using the piston splitter. The pattern with the column spacing of 1.0 m is the optimal choice of hole network layout scheme, after analyzing the splitting force evolution over the piston travel of the splitter.

(4) The preliminary field test of mechanical fracturing excavation technology was conducted in a parking chamber in the Kalatongke Mine, where the initial cut was constructed through the core drilling rig. And when the hole margin is 1.0–1.5 m, the roadway excavation with mechanical fracturing is feasible, with footage of 0.8 m. Therefore, the reasonable fracturing hole margin is about 1.0 m.

Data Availability

The data that support the findings of this study are available from the corresponding author, D. Huang, upon reasonable request.

Conflicts of Interest

The authors declare that they have no conflicts of interest.

Authors' Contributions

Yin Chen is responsible for the methodology; Dan Huang is responsible for the project administration; Zijun Li is responsible for the supervision of the study; Jian Zhao is responsible for writing—original draft.

Acknowledgments

This work was supported by the National Key Research and Development Program of China (No. 2021YFC2902102).

References

[1] S. Xu, Y. Li, J. Liu, and F. Zhang, "Optimization of blasting parameters for an underground mine through prediction of blasting vibration," *Journal of Vibration and Control*, vol. 25, no. 9, pp. 1585–1595, 2019.

[2] Y. Ghorbani, G. T. Nwaila, S. E. Zhang et al., "Moving towards deep underground mineral resources: drivers, challenges and potential solutions," *Resources Policy*, vol. 80, Article ID 103222, 2023.

[3] S. Ibarra-Gutiérrez, J. Bouchard, M. Laflamme, and K. Fytas, "Project economics of lithium mines in Quebec: a critical review," *The Extractive Industries and Society*, vol. 8, no. 4, Article ID 100984, 2021.

[4] M. E. Yetkin, "Examining of rock drilling properties in underground metal mine excavation," *Anais da Academia Brasileira de Ciências*, vol. 93, no. 1, 2021.

[5] H. K. Verma, N. K. Samadhiya, M. Singh, V. V. R. Prasad, and R. K. Goel, "Investigations of rockmass damage induced by blasting in tunnelling," *Journal of Rock Mechanics & Tunnelling Technology (JRMTT)*, vol. 22, no. 1, pp. 49–61, 2016.

[6] H. M. An, H. Y. Liu, H. Han, X. Zheng, and X. G. Wang, "Hybrid finite-discrete element modelling of dynamic fracture and resultant fragment casting and muck-piling by rock blast," *Computers and Geotechnics*, vol. 81, pp. 322–345, 2017.

[7] P. LI and M.-F. CAI, "Challenges and new insights for exploitation of deep underground metal mineral resources," *Transactions of Nonferrous Metals Society of China*, vol. 31, no. 11, pp. 3478–3505, 2021.

[8] X. Tan, W. Chen, H. Liu et al., "A combined supporting system based on foamed concrete and U-shaped steel for underground coal mine roadways undergoing large deformations," *Tunnelling and Underground Space Technology*, vol. 68, pp. 196–210, 2017.

[9] H. K. Verma, N. K. Samadhiya, M. Singh, R. K. Goel, and P. K. Singh, "Blast induced rock mass damage around tunnels," *Tunnelling and Underground Space Technology*, vol. 71, pp. 149–158, 2018.

[10] H. Sun, Y. Liu, T. Jiang, T. Liu, and D. Liu, "Application of dust control method based on water medium humidification in tunnel drilling and blasting construction environment," *Building and Environment*, vol. 234, Article ID 110111, 2023.

[11] S. Xu, T. Chen, J. Liu, C. Zhang, and Z. Chen, "Blasting vibration control using an improved artificial neural network in the ashele copper mine," *Shock and Vibration*, vol. 2021, Article ID 9949858, 11 pages, 2021.

[12] A. Pomasoncco-Najarro, C. Trujillo-Valerio, L. Arauzo-Gallardo, C. Raymundo, G. Quispe, and F. Dominguez, "Pre-split blasting design to reduce costs and improve safety in underground mining," *Energy Reports*, vol. 8, pp. 1208–1225, 2022.

[13] Q. Qian and P. Lin, "Safety risk management of underground engineering in China: progress, challenges and strategies," *Journal of Rock Mechanics and Geotechnical Engineering*, vol. 8, no. 4, pp. 423–442, 2016.

[14] W. Mao, W. Wang, H. Sun, and D. Luo, "Barriers to implementing the strictest environmental protection institution: a multi-stakeholder perspective from China," *Environmental Science and Pollution Research*, vol. 27, no. 31, pp. 39375–39390, 2020.

[15] X. Li, K. Liu, T. Qiu, Y. Sha, J. Yang, and R. Song, "Numerical study on fracture control blasting using air–water coupling," *Geomechanics and Geophysics for Geo-Energy and Geo-Resources*, vol. 9, Article ID 29, 2023.

[16] S. Liu, H. Ji, D. Han, and C. Guo, "Experimental investigation and application on the cutting performance of cutting head for rock cutting assisted with multi-water jets," *The International Journal of Advanced Manufacturing Technology*, vol. 94, pp. 2715–2728, 2018.

[17] F. Li, H. Liu, G. Xiang, B. Ren, Y. Zou, and R. Sun, "The numerical simulation of rapid excavation technologies under the combined form of hydraulic fracturing and drill-and-blast method," *Journal of Building Engineering*, vol. 73, Article ID 106757, 2023.

[18] A. Al-Bakri and M. Hefni, "A review of some nonexplosive alternative methods to conventional rock blasting," *Open Geosciences*, vol. 13, no. 1, pp. 431–442, 2021.

[19] G. A. Cooper, J. Berlie, and A. Merminod, "A novel concept for a rock-breaking machine. II. Excavation techniques and experiments at larger scale," *Proceedings of the Royal Society a Mathematical, Physical and Engineering Sciences*, vol. 373, pp. 353–372, 1980.

[20] S. J. Anderson, "Drill-split mining with radial-axial loading splitters," in *Rock Mechanics Contributions and Challenges*, W. Hustrulid and G. A. Johnson, Eds., pp. 511–518, CRC Press, 1st edition, 1990.

[21] H. Li, S. Liu, G. Cheng, and C. Guo, "Numerical investigation on rock-fracturing mechanism by using splitter under hole assistance," *Shock and Vibration*, vol. 2019, Article ID 4395729, 14 pages, 2019.

[22] S. Liu, H. Li, and G. Cheng, "Numerical and experimental investigation on rock breaking performance with hydraulic splitter," *Tunnelling and Underground Space Technology*, vol. 96, Article ID 103181, 2020.

[23] F. Zhou, S. Liu, J. Huang, and S. Cui, "Experimental investigation of the fracture performance of hard rock with a single borehole by using a hydraulic splitter," *Arabian Journal for Science and Engineering*, vol. 46, no. 11, pp. 10655–10666, 2021.

[24] W. W. de Graaf and W. Spiteri, "A preliminary qualitative evaluation of a hydraulic splitting cylinder for breaking rock in deep-level mining," *Journal of the Southern African Institute of Mining and Metallurgy*, vol. 118, no. 8, 2018.

[25] R.-S. Yang, X.-H. Zhang, Z.-R. Zhang, and X.-S. Bai, "Application of slotting-pipe shaped blasting for hard-rock rapid driving," *Journal of Coal Science and Engineering*, vol. 19, no. 2, pp. 143–146, 2013.